THE ROYAL SOCIETY

A minimal mechanism for bacterial pattern formation

R. Tyson[1], S. R. Lubkin[2] and J. D. Murray[1]

[1]*Department of Applied Mathematics, Box 352420, University of Washington, Seattle, WA 98195-2420, USA*
[2]*Biomathematics Program and Departments of Statistics and of Mathematics, Box 8203, North Carolina State University, Raleigh, NC 27695-8203, USA*

Colonies of *Escherichia coli* or *Salmonella typhimurium* form geometrically complex patterns when exposed to, or feeding on, intermediates of the tricarboxylic acid (TCA) cycle. In response to the TCA cycle intermediate, the bacteria secrete aspartate, a potent chemo-attractant. As a result, the cells form high-density aggregates arranged in striking regular patterns. The simplest are temporary spots formed in a liquid medium by both *E. coli* and *S. typhimurium*. In semi-solid medium *S. typhimurium* forms concentric rings arising from a low-density bacterial lawn, which are either continuous or spotted, whereas *E. coli* forms complex patterns arising from a dense swarm ring, including interdigitated spots (also called sunflower spirals), radial spots, radial stripes and chevrons. We present a mathematical model that captures all three of the pattern-forming processes experimentally observed in both *E. coli* and *S. typhimurium*, using a minimum of assumptions.

Keywords: chemotaxis; bacterial patterns; mathematical modelling; bacterial aggregates; spots; stripes

1. INTRODUCTION

Colonies of *Escherichia coli* or *Salmonella typhimurium* form geometrically complex patterns when exposed to, or feeding on, intermediates of the tricarboxylic acid (TCA) cycle (Budrene & Berg 1991, 1995). In response to the TCA cycle intermediate, the bacteria secrete aspartate, which is a potent chemo-attractant. Subsequently, the cells form high-density aggregates arranged in a regular pattern, by means of at least three very different pattern-forming processes, each of which will be described below.

Although each pattern-forming process is unique, the essential elements of bacteria, aspartate (chemo-attractant) and TCA cycle intermediate (pattern stimulant) remain the same. Among the pattern stimulants, succinate and fumarate produced the strongest effect (Budrene & Berg 1991). In the following, we refer to the TCA cycle intermediate as succinate, although fumarate is understood to be equivalent for our purposes.

In bacterial chemotaxis, exactly how the complex arrangements form from interactions between individuals is difficult to determine. In cases such as this, when biological intuition seems unable to provide an adequate explanation, mathematical modelling can play an especially helpful role. Since the pioneering study by Keller & Segel (1971*a*,*b*), a considerable amount of modelling effort has been expended on these patterns. Ben-Jacob *et al*. (1995) and Tsimring *et al*. (1995) had thresholding behaviour in aspartate production and a cell-secreted waste field in their model. They obtained spatial patterns resembling some of the experimentally observed *E. coli* patterns. Bruno (1992) assumed constant chemo-attractant production and obtained interesting patterns. Brenner *et al*. (1998) performed a one-dimensional analysis of the swarm ring mechanism in the formation of *E. coli* patterns in semi-solid medium. They studied the relative importance of the terms in their model from the point of view of pattern formation. Their conclusions are consistent with our two-dimensional results. Woodward *et al*. (1995), modelling the *S. typhimurium* patterns in semi-solid medium, assumed degradation rather than uptake of aspartate. It has subsequently become clear (Budrene & Berg 1995) that the cells do consume aspartate and that the chemical is very stable and does not degrade on its own.

All of these models contain more or less reasonable assumptions, and produce interesting patterns, yet none has been studied with respect to all three pattern-forming processes, when any realistic model of the system must reproduce them all. In this paper we present a mathematical model that captures all three observed pattern-forming processes based on a minimum of assumptions.

We briefly mention here some related models by Kawasaki *et al*. (1997). In their paper, they model non-chemotactic bacterial patterns formed by the bacteria *Bacillus subtilis*. Their model is a reaction–diffusion system with density-dependent diffusion instead of chemotaxis (negative density-dependent diffusion) as we have. The dendritic patterns produced by *Bacillus* and by Kawasaki *et al*. are very different from ours. Other interesting patterns *in vitro*, in fungi, have been modelled by Davidson *et al*. (1996).

2. MATHEMATICAL MODEL

Combining the key biological processes into a mathematical model, we write a system of three conservation equations of the form

Received 17 August 1998 *Accepted* 15 October 1998

$$\boxed{\text{rate of change of cell density } n} = \boxed{\text{random migration of cells}} + \boxed{\text{chemotaxis of cells to aspartate}} + \boxed{\text{growth and death of cells}}$$

$$\boxed{\text{rate of change of aspartate concentration } c} = \boxed{\text{diffusion of aspartate}} + \boxed{\text{production of aspartate by cells}} - \boxed{\text{uptake of aspartate by cells}}$$

$$\boxed{\text{rate of change of succinate concentration } s} = \boxed{\text{diffusion of succinate}} - \boxed{\text{uptake of succinate by cells}} \qquad (1)$$

where n denotes bacterial cell density, c the aspartate concentration and s the succinate concentration.

Experimental justification of various functional forms is available for many of the boxed terms. Below, we will discuss first the diffusion and random migration terms, then the chemotaxis term, and finally the four reaction terms in increasing order of complexity.

The diffusion terms are straightforward, as aspartate and succinate undergo classical Fickian diffusion. The bacteria do not strictly diffuse, but careful study of their motion indicates that they do perform a random walk. At the population level, then, the bacteria can also be thought of as substances diffusing in a Fickian manner (Berg 1983; Berg & Turner 1990); diffusion coefficients have been measured (Phillips *et al.* 1994).

The chemotactic flux of *E. coli* in the presence of fixed aspartate gradients was measured by Dahlquist & Lovely (1972) and a mathematical expression was derived from these experiments by Lapidus & Schiller (1976) (see Ford & Lauffenburger (1991) for a review). The two bacteria *E. coli* and *S. typhimurium* are very closely related, and so it is safe to assume that their chemotactic response to aspartate is very similar. Thus we have the chemotaxis flux term

$$\frac{k_1 n}{(k_2 + c)^2} \nabla c, \qquad (2)$$

where k_1 and k_2 are known (table 1). The implication of the density-dependent term is that the chemotactic flux decreases as the background level of chemo-attractant increases.

Of the reaction terms, the simplest are the uptake of aspartate and uptake of succinate terms. We assume that uptake of aspartate occurs simply at a rate proportional to the aspartate concentration. Thus we have $u(c) = k_7 c$ for consumption of aspartate, where k_7 is the rate constant. Consumption of succinate is proportional to population growth rate (see below), with proportionality constant k_8, because the cells are converting nutrient to cells.

The terms for proliferation (growth and death) of cells and production of aspartate are less easily selected. We can show that the exact functional form of each of these terms is not critical. Budrene & Berg (1995) observe that the cell density achieved in a Petri dish after some unspecified amount of time depends on the amount of nutrient initially available. For these experiments, the pattern stimulant, succinate, is also the main nutrient. So we know that growth rate per cell increases with initial concentration of succinate. At any given concentration of succinate, the growth rate per cell is constant (Budrene & Berg 1995). This gives $nb(s)$ for the population growth rate, where $b(s)$ is a monotonically increasing function of s that levels off as succinate concentration increases. For the simulations presented in this paper, we used $b(s) = k_3 k_4 s^2/(k_9 + s^2)$.

Table 1. *Dimensional parameter values obtained from the literature for use in the* E. coli *and* S. typhimurium *model equations (4)*

parameter	value	source
k_1	3.9×10^{-9} M cm^2 s^{-1}	Dahlquist *et al.* 1972
k_2	5×10^{-6} M	Dahlquist *et al.* 1972
D_n	$2\text{–}4 \times 10^{-6}$ cm^2 s^{-1}	Berg & Turner 1990; Berg 1983, p. 93
D_c	8.9×10^{-6} cm^2 s^{-1}	Berg 1983
D_s	$\approx 9 \times 10^{-6}$ cm^2 s^{-1}	Berg 1983
n_0	10^8 cells ml^{-1}	Budrene & Berg 1991
s_0	$1\text{–}3 \times 10^{-3}$ M	Budrene & Berg 1995

The death rate $d(n,s)$ per cell, corresponding to cells becoming non-motile, is unknown. Some plausible assumptions are a constant death rate $d(n,s) = -k_3$, and/or a death rate that increases with high cell densities, $d(n,s) = -k_3 n$, where k_3 is constant. For the simulations presented in this paper, we used the latter.

For the production of aspartate per cell, $p(n,s)$, we know that the presence of a TCA cycle intermediate is necessary, so $p(n,0) = 0$. We also know from experiment (Budrene & Berg 1995) that the amount of aspartate produced increases with the amount of succinate present. Thus aspartate production is an increasing function of succinate concentration. For the model to yield pattern, analysis (Tyson *et al.* 1998*a*,*b*) shows that the production of aspartate must increase sufficiently quickly at low succinate concentrations. The behaviour of the function at larger concentrations of succinate is not critical. A number of functions were tested, and for the results presented in this paper we used $p(n,s) = k_5 s n/(k_6 + n^2)$. This is a saturating function of cell density indicating that, as cell density increases, production of chemo-attractant decreases. It would be more usual to have Michaelis–Menten kinetics, with the cell density dependence being $1/(k_6 + n)$. Here we find we need the order n^2 dependence for sufficiently rapid increase in production of aspartate at low succinate concentrations.

Collecting all of the information just presented, we have

$$\begin{aligned} u_c(c) &= k_7 c \\ u_s(s) &= k_8 \frac{k_4 s^2}{k_9 + s^2} \\ p(n,s) &= k_5 s \frac{n}{k_6 + n^2} \\ b(s) &= k_3 \frac{k_4 s^2}{k_9 + s^2} \\ d(n,s) &= k_3 n \end{aligned} \qquad (3)$$

for uptake of aspartate, uptake of succinate, aspartate production, cell birth and cell death. Because each of these functions is behaviour per cell, they each must be multiplied by n in our equations.

We thus arrive at the mathematical representation of the model system (1):

$$\begin{aligned}\frac{\partial n}{\partial t} &= D_n\nabla^2 n - \nabla\left[\frac{k_1 n}{(k_2+c)^2}\nabla c\right] + k_3 n\left(\frac{k_4 s^2}{k_9+s^2} - n\right)\\ \frac{\partial c}{\partial t} &= D_c\nabla^2 c + k_5 s\frac{n^2}{k_6+n^2} - k_7 nc \qquad (4)\\ \frac{\partial s}{\partial t} &= D_s\nabla^2 s - k_8 n\frac{k_4 s^2}{k_9+s^2}\ .\end{aligned}$$

Known parameter values are listed in table 1. For numerical simulations, we used a fractional step method with 'Strang splitting' as discussed in Tyson *et al.* (1998*b*). The simulations were done on non-dimensionalized equations as detailed in Tyson *et al.* (1999), with zero-flux boundary conditions. The initial conditions for the liquid-medium simulations were $n(x,y) = n_0$, $c(x,y) = 0$ and $s(x,y) = s_0$. For the semi-solid *S. typhimurium* and *E. coli* simulations the initial conditions were

$$\begin{aligned}n(r) &= n_0 f(r) \ \text{ for } \ r \leqslant R\\ &= 0 \ \text{ for } \ r > R c(x,y) = 0 \qquad (5)\\ &\qquad s(x,y) = s_0,\end{aligned}$$

where $r = \sqrt{(x^2+y^2)}$ and $f(r)$ is a radially symmetric bell-shaped function with local support centred at the origin. The outer limit of the cell inoculum, R, was chosen to be small compared with the size of the simulation domain. The grid size used varied from 150×150 points to 300×300 points. Actual values for each figure are given in the figure captions.

3. PATTERNS FORMED IN LIQUID MEDIUM

The liquid medium patterns were briefly described by Budrene & Berg (1991). Initially, succinate is uniformly added to a thin, well-stirred layer of liquid medium containing bacteria. Aggregates form randomly over the entire surface after a short interval. The aggregates are separated by regions of near-zero cell density, and coalesce with other aggregates to form fewer and larger ones. The pattern eventually disappears, after which it cannot be induced to re-form.

The patterns arise and disappear in less than a generation time, so proliferation of cells is not involved and we set k_3 to zero. The liquid medium contains sufficient nutrients for the bacteria so that they do not consume significant quantities of succinate or aspartate, so we set $k_7 = k_8 = 0$ and assume that s is spatially uniform. The equations for the liquid experiments are therefore a special case of the general equations (4). The simplified system is

$$\begin{aligned}\frac{\partial n}{\partial t} &= D_n\nabla^2 n - \nabla\left[\frac{k_1 n}{(k_2+c)^2}\nabla c\right];\\ \frac{\partial c}{\partial t} &= D_c\nabla^2 c + k_5 s\frac{n^2}{k_6+n^2}.\end{aligned}$$

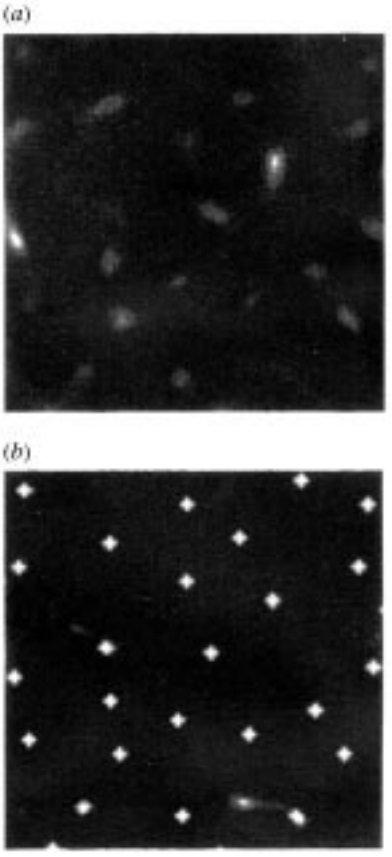

Figure 1. Liquid medium model with succinate added uniformly, simulation results. White corresponds to high cell density, black to low density. Parameter cell values: $D_n/D_c = 0.25$, $k_1/D_c k_2 = 90$, $k_6/n_0^2 = 100$.

Because the chemo-attractant is produced and not consumed, the concentration of aspartate in the Petri dish increases with time. This leads to saturation of the chemotaxis term, until eventually diffusion is the dominant spatial process. Thus we can immediately see that any pattern which initially forms will eventually disappear, as is observed experimentally and can be shown analytically (Tyson *et al.* 1998*a*).

Numerical results are shown in figure 1. Aggregates form in response to the stimulant, initially as faint threads and then as distinct spots. The pattern wavelength (distance between spots) increasing as aggregates coalesce and their numbers decrease. On the bottom right-hand corner of figure 1*b* two spots can be seen coalescing. After a sufficiently long time (not shown) (Tyson *et al.* 1998*a*), the pattern disappears.

4. *S. TYPHIMURIUM* PATTERNS IN SEMI-SOLID MEDIUM

S. typhimurium forms relatively simple patterns in semi-solid medium (Woodward *et al.* 1995). Initially succinate is uniformly distributed throughout a thin layer of semi-solid medium (0.24% water agar), and an inoculum of cells is added to the centre.

After addition of cells, a low-density bacterial lawn spreads radially from the initial inoculum. Some time later, a high-density ring of bacteria appears at a radial distance less than the radius of the lawn. After another

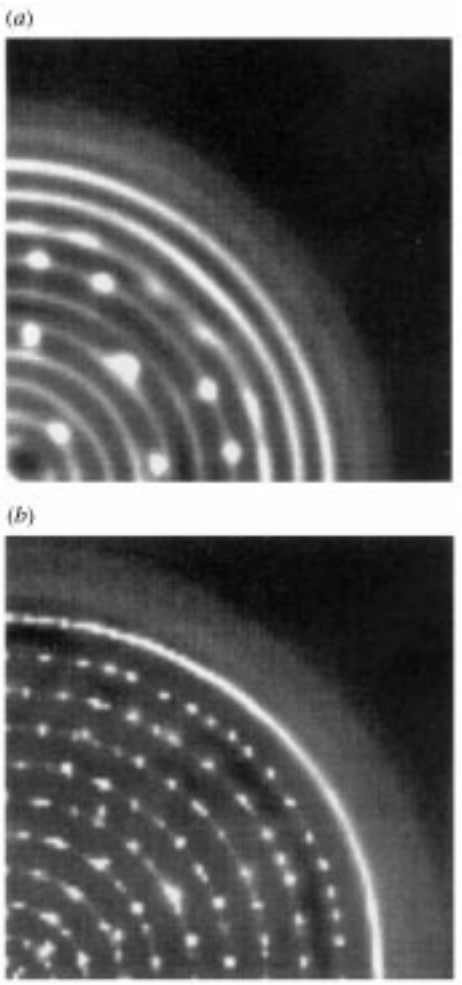

Figure 2. Semi-solid medium model, simulation results, *S. typhimurium* patterns: (*a*) concentric rings (transition to spotted rings pattern) and (*b*) concentric spotted rings. White indicates high cell density, black the opposite. Parameter values: (*a*) $D_n/D_c = 0.25$, $D_s/D_c = 0.89$, $k_1/k_2D_c = 40$, $k_3/k_7 = 1.0$, $k_4/n_0 = 70$, $k_5\sqrt{k_9}/k_7k_2n_0 = 10$, $k_8/k_7\sqrt{k_9} = 5 \times 10^{-3}$, $k_6/n_0^2 = 100$. (*b*) $D_n/D_c = 0.26$, $D_s/D_c = 0.89$, $k_1/k_2D_c = 89$, $k_3/k_7 = 1.0$, $k_4/n_0 = 7$, $k_5\sqrt{k_9}/k_7k_2n_0 = 8$, $k_8/k_7\sqrt{k_9} = 1 \times 10^{-3}$, $k_6/n_0^2 = 100$.

time interval, when the lawn has expanded further, a second high density bacterial ring appears at some radius larger than that of the first ring. The rings, once formed, are stationary. This process continues until the Petri dish is full of rings.

The rings may remain continuous, or may break up to become rings of spots. The high-density aggregates in one ring bear no obvious positional relation to the aggregates in the two neighbouring rings, and spots are closer within a ring than between rings. The patterns form slowly in these experiments, over a period of 2–3 days. The generation time is 2 h, and so proliferation is important. Consumption of aspartate and succinate also occur. The equations for these experiments are thus the full system (4).

Numerical simulations are shown in figure 2*a*,*b*. Qualitatively, the simulation results correspond well to the experimental results. The numerical pattern is preceded by a bacterial lawn of low cell density. Each ring forms at a consistent radial distance from the previous one, and then remains stationary. The spotted rings form first as continuous rings, which subsequently break up into spots. The distance between spots in a ring is affected by the ratio k_6/n_0^2. As this ratio increases, the distance between spots within a ring decreases (Tyson *et al*. 1999) so we conclude that the chemo-attractant production term is strongly dependent on n at low bacterial densities.

Some quantitative comparison between the model and experiment is possible. Taking the parameter values from figure 2, we find that four rings form in a distance $x = 1.4$ cm. This is close to the experimentally observed value of $x \approx 1$ cm (Woodward *et al*. 1995). Owing to the fact that a number of model parameters are unknown, we do not know what the dimensional time is. The times taken for the first four rings to form experimentally and numerically are not comparable, because the density and distribution of cells at the inoculum affect the time for formation of the first ring.

5. *E. COLI* PATTERNS IN SEMI-SOLID MEDIUM

The most spectacular patterns are exhibited by *E. coli* in a semi-solid medium. The experimental situation is exactly the same as for the *S. typhimurium* patterns, but the process whereby pattern forms is very different. Initially, instead of a thin bacterial lawn, a swarm ring (high-density ring of vigorously motile bacteria) forms and expands outwards from the initial inoculum. The bacterial density in the swarm ring increases until some point at which the ring becomes unstable, and some percentage of the bacteria are left behind as aggregates. These aggregates remain bright (full of vigorously motile bacteria) for a short period of time, but then dissolve as the bacteria rejoin the swarm ring. Left behind in the aggregate's original location is a clump of bacteria, which, for some reason as yet unknown, are non-motile. These non-motile bacteria remain as markers of the pattern.

Radial and tangential distances between spots are comparable, and in the final pattern there exists a definite positional relation between radially and tangentially neighbouring aggregates. This relation appears to be the result of existing aggregates inducing the formation of subsequent ones (Budrene & Berg 1995). The speed of the swarm ring and the time at which the dissolution of aggregates occurs are likely to be key elements in the formation of any one pattern. If the dissolution happens quickly, the aggregates appear to be pulled along by the swarm ring, and the non-motile bacteria are left behind as a radial streak. If the dissolution happens less quickly, the cells from the dissolved aggregate rejoin the swarm ring and induce the formation of aggregates at the rejoining locations. This results in a pattern of radial spots. If the dissolution happens even more slowly, the swarm ring becomes unstable before the bacteria from the aggregates have time to rejoin the ring. The ring then tends to form aggregates in between the locations where aggregates already exist. This results in an interdigitated-spots type of pattern, approximating hexagonal symmetry.

As in the *S. typhimurium* experiments, proliferation of cells and consumption of aspartate and succinate are important, so we model these experiments with the full model, equations (4).

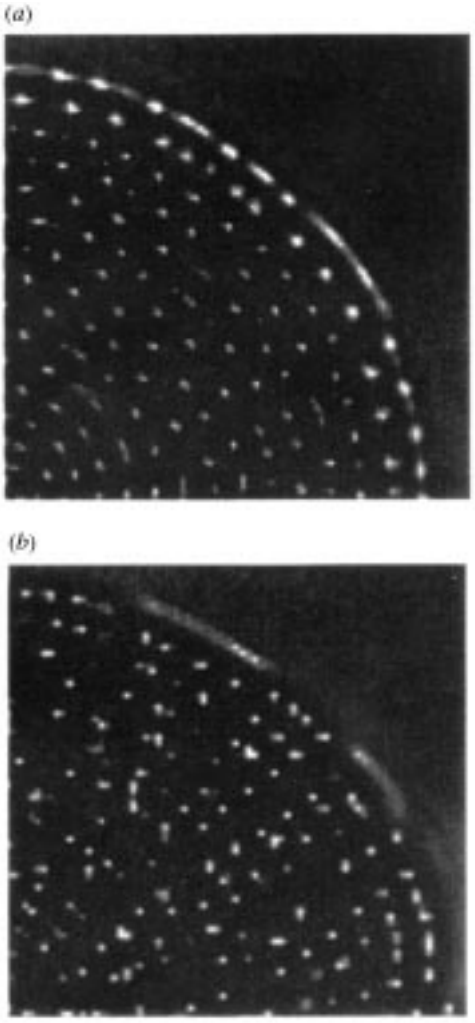

Figure 3. Semi-solid medium model, simulation results, *E. coli* patterns: (*a*) interdigitated spots, (*b*) radial spots. White indicates high cell density, black the opposite. Parameter values: (*a*) $D_n/D_c = 0.25$, $D_s/D_c = 0.89$, $k_1/k_2D_c = 89$, $k_3/k_7 = 1.0$, $k_4/n_0 = 7$, $k_5\sqrt{k_9}/k_7k_2n_0 = 32$, $k_8/k_7\sqrt{k_9} = 0.20$, $k_6/n_0^2 = 100$. (*b*) $D_n/D_c = 0.25$, $D_s/D_c = 1.0$, $k_1/k_2D_c = 90$, $k_3/k_7 = 1.0$, $k_4/n_0 = 3.5$, $k_5\sqrt{k_9}/k_7k_2n_0 = 29$, $k_8/k_7\sqrt{k_9} = 1 \times 10^{-2}$, $k_6/n_0^2 = 49$.

Simulation and analysis (R. Tyson, S. Lubkin and J. D. Murray, unpublished data) show that the model yields a swarm ring, which leaves rings of spots behind. Following the experimental paradigm, we take the same parameters just studied and increase the amount of nutrient present. Numerical results are again consistent with experiment and show that increased nutrient results in more spots per unit length following the swarm ring. The change also increases the cell density in the swarm ring and in the spots themselves, and the spots remain visible for a greater length of time.

We have obtained an interdigitated-spots pattern and a radial-spots pattern (figure 3) which are qualitatively similar to the experimental ones. The regular pattern does not begin until some critical radius. The pattern observed experimentally under phase-contrast microscopy is devoid of cells toward the centre, whereas the simulation contains a random arrangement of a few aggregates.

Our non-dimensionalization (R. Tyson, S. Lubkin and J. D. Murray, unpublished data) allows us to make a quantitative comparison between the model and experiment. We have

$$\frac{t^*}{(x^*)^2} = D_c\frac{t}{x^2},$$

where t^* and x^* are the dimensionless time and distance units, respectively. Taking x^* as the distance between neighbouring rings, and t^* as the time taken to form a neighbouring ring, we have found this ratio to range from 0.1 to 0.04 (its value in figure 3) in our simulations. These results compare reasonably well with the experimental value, which is approximately 0.2.

6. CONCLUSIONS

There are many encouraging similarities between the results of the model and those of the experiment. We have found that the model can exhibit all three pattern forming processes observed in experiment. These are (i) the temporary formation of aggregates in liquid medium, (ii) the formation of a thin bacterial lawn and subsequently stationary rings of *S. typhimurium* in semi-solid medium, and (iii) a swarm ring spawning regularly spaced aggregates of *E. coli* in semi-solid medium. In addition, we also find that the patterns produced by each process include many similarities to the patterns observed experimentally, including the radial spots and interdigitated spots of the *E. coli* repertoire.

With a minimal set of assumptions, we have built a model that captures many of the essential characteristics of the experiments. In future, as our understanding of the experiments increases, an improved model should eventually encompass all of their salient features. Two obvious candidates for further investigation are the nutrient concentration as bifurcation parameter for the semi-solid medium patterns, and the two remaining *E. coli* geometries, radial stripes and chevrons.

With the present model we have already seen some radial travel by the swarm-ring aggregates. This phenomenon experimentally gives rise to the radial streaks in the radial stripes and chevron patterns. In our simulations, we find this behaviour at higher nutrient concentrations and higher swarm-ring speeds than we have been considering thus far, so their study will require a larger grid and considerably more computation.

This work has been supported in part by NSF grants DMS-9306108 (S.R.L.) and DMS-9500766 (S.R.L., J.D.M.), and by NSERC scholarships PGSA and PGSB (R.T.).

REFERENCES

Ben-Jacob, E., Cohen, I., Schochet, O., Aranson, I., Levine, H. & Tsimring, L. 1995 Complex bacterial patterns. *Nature* **373**, 566–567.

Berg, H. C. 1983 *Random walks in biology.* Princeton University Press.

Berg, H. C. & Turner, L. 1990 Chemotaxis of bacteria in glass capillary arrays. *Biophys. J.* **58**, 919–930.

Brenner, M. P., Levitov, L. S. & Budrene, E. O. 1998 Physical mechanisms for chemotactic pattern formation by bacteria. *Biophys. J.* (In the press.)

Bruno, W. J. 1992 Patterns that grow. *CNLS Newslett.* **82**, 1–10.

Budrene, E. O. & Berg, H. C. 1991 Complex patterns formed by motile cells of *Escherichia coli*. *Nature* **349**, 630–633.

Budrene, E. O. & Berg, H. C. 1995 Dynamics of formation of symmetrical patterns by chemotactic bacteria. *Nature* **376**, 49–53.

Dahlquist, F. W., Lovely, P. & Koshland, D. E. Jr 1972 Qualitative analysis of bacterial migration in chemotaxis. *Nature, New Biol.* **236**, 120–123.

Davidson, F. A., Sleeman, B. D., Rayner, A. D. M., Crawfore, J. W. & Ritz, K. 1996 Context-dependent macroscopic patterns in growing and interacting mycelial networks. *Proc. R. Soc. Lond.* B **263**, 873–880.

Ford, R. M. & Lauffenberger, D. A. 1991 Analysis of chemotactic bacterial distributions in population migration assays using a mathematical model applicable to steep or shallow attractant gradients. *Bull. Math. Biol.* **53**, 721–749.

Kawasaki, K., Mochizuki, A., Matsushita, M., Umeda, T. & Shigesada, N. 1997 Modeling spatio-temporal patterns generaged by *Bacillus subtilis*. *J. Theor. Biol.* **188**, 177–185.

Keller, E. F. & Segel, L. A. 1971*a* Model for chemotaxis. *J. Theor. Biol.* **30**, 225–234.

Keller, E. F. & Segel, L. A. 1971*b* Travelling bands of chemotactic bacteria: a theoretical analysis. *J. Theor. Biol.* **30**, 235–248.

Lapidus, R. & Schiller, R. 1976 Model for the chemotactic response of a bacterial population. *Biophys. J.* **16**, 779–789.

Phillips, B. R., Quinn, J. A. & Goldfine, H. 1994 Random motility of swimming bacteria: single cells compared to cell-populations. *A. I. Ch. E. Jl* **40**, 334–348.

Tsimring, L., Levine, H., Aranson, I., Ben-Jacob, E., Cohen, I. & Schochet, O. 1995 Aggregation patterns in stressed bacteria. *Phys. Rev. Lett.* **75**, 1859–1862.

Tyson, R., Lubkin, S. R. & Murray, J. D. 1998*a* Model and analysis of chemotactic bacterial patterns in liquid medium. *J. Math. Biol.* (In the press.)

Tyson, R., Stern, L. G. & LeVeque, R. J. 1998*b* Fractional step methods applied to a chemotaxis model. *J. Math. Biol.* (In the press.)

Tyson, R., Lubkin, S. R. & Murray J. D. 1999 Analysis of chemotactic *Salmonella typhimurium* patterns in a semi-solid medium. *SIAM J. Appl. Math.* (Submitted.)

Woodward, D. E., Tyson, R., Myerscough, M. R., Murray, J. D., Budrene, E. O. & Berg, H. C. 1995 Spatio-temporal patterns generated by *Salmonella typhimurium*. *Biophys. J.* **68**, 2181–2189.